THE JOURNAL OF BIOLOGICAL CHEMISTRY
Vol. 279, No. 33, Issue of August 13, pp. 35037–35046, 2004

Printed in U.S.A.

Lipoprotein Receptor Binding, Cellular Uptake, and Lysosomal Delivery of Fusions between the Receptor-associated Protein (RAP) and α-L-Iduronidase or Acid α-Glucosidase*

Received for publication, March 8, 2004, and in revised form, May 5, 2004
Published, JBC Papers in Press, May 31, 2004, DOI 10.1074/jbc.M402630200

William S. Prince‡, Lynn M. McCormick§, Dan J. Wendt‡, Paul A. Fitzpatrick‡, Keri L. Schwartz‡, Allora I. Aguilera‡, Vishwanath Koppaka‡, Terri M. Christianson‡, Michel C. Vellard‡, Nadine Pavloff‡, Jeff F. Lemontt‡, Minmin Qin‡, Chris M. Starr‡, Guojun Bu§¶, and Todd C. Zankel‡‖

From ‡BioMarin Pharmaceutical, Inc., Novato, California 94949 and the §Departments of Pediatrics, Cell Biology and Physiology, Washington University School of Medicine, St. Louis, Missouri 63110

Enzyme replacement therapy for lysosomal storage disorders depends on efficient uptake of recombinant enzyme into the tissues of patients. This uptake is mediated by oligosaccharide receptors including the cation-independent mannose 6-phosphate receptor and the mannose receptor. We have sought to exploit alternative receptor systems that are independent of glycosylation but allow for efficient delivery to the lysosome. Fusions of the human lysosomal enzymes α-L-iduronidase or acid α-glucosidase with the receptor-associated protein were efficiently endocytosed by lysosomal storage disorder patient fibroblasts, rat C6 glioma cells, mouse C2C12 myoblasts, and recombinant Chinese hamster ovary cells expressing individual members of the low-density lipoprotein receptor family. Uptake of the fusions exceeded that of phosphorylated enzyme in all cases, often by an order of magnitude or greater. Uptake was specifically mediated by members of the low-density lipoprotein receptor protein family and was followed by delivery of the fusions to the lysosome. The advantages of the lipoprotein receptor system over oligosaccharide receptor systems include more efficient cellular delivery and the potential for transcytosis of ligands across tight endothelia, including the blood-brain barrier.

Enzyme replacement therapy for lysosomal storage disorders relies on the efficient delivery of recombinant enzyme to all of the affected tissues of the patient (1). Uptake of enzyme from the blood following intravenous administration requires specific oligosaccharides on the enzyme itself and corresponding oligosaccharide receptors on target cells. Examples include the binding of phosphorylated high-mannose oligosaccharides on α-L-iduronidase by the cation-independent mannose 6-phosphate receptor (MPR)[1] and binding of high-mannose oligosaccharides on glucocerebrosidase by the mannose receptor (2, 3). The former system is the basis for treatment of patients with Hurler syndrome, the latter for Gaucher syndrome. Factors that limit uptake by these systems include the extent to which the recombinant enzyme is modified with the necessary oligosaccharides and the density of the oligosaccharide receptors on different tissues. The absence of quality control mechanisms for oligosaccharide modifications in the secretory pathway can lead to poorly modified recombinant enzymes. This deficiency has been addressed, with varying success, by post-secretory modification of recombinant enzymes with glycosidases or glycosyltransferases (4). Another solution to the problem is to utilize alternative uptake mechanisms that rely on protein-based, rather than oligosaccharide-based, targeting determinants. Some studies have focused on the use of small, basic peptides, like human immunodeficiency virus TAT, for this purpose (5, 6). Others have demonstrated the feasibility of this approach using insulin-like growth factor-2, a peptide ligand for the MPR (7).

The low density lipoprotein receptor (LDLR) family is one of the most widely distributed and intensively utilized receptor types in the body (8–11). The LDLR family consists of a diverse group of trans-membrane, cell-surface receptors that bind to a wide variety of different ligands. A number of LDLR family members, including the LDLR-related protein 1 (LRP1) and megalin/LRP2, are professional endocytic receptors that mediate uptake of bound ligands into cells with subsequent delivery to the lysosome (12). Megalin also mediates transcytosis of some of its ligands across epithelial cell layers, including the brain capillary endothelium, kidney proximal tubule epithelium, and thyroid epithelium (13–16).

All members of the LDLR family except for LDLR itself are bound with high affinity by the receptor-associated protein (RAP), a 39-kDa resident of the endoplasmic reticulum (17–19). RAP acts as a chaperone, preventing association of LDLR family members with their physiological ligands in the secretory pathway, a function that permits proper folding of the receptors prior to their transport to the cell surface. LRP ligand-binding domains are made up of arrays of cysteine-rich, calcium-binding modules called complement-type repeats (20, 21).

* The costs of publication of this article were defrayed in part by the payment of page charges. This article must therefore be hereby marked "*advertisement*" in accordance with 18 U.S.C. Section 1734 solely to indicate this fact.

¶ Supported by grants from BioMarin Pharmaceutical and the National Institutes of Health.

‖ To whom correspondence should be addressed. E-mail: tzankel@bmrn.com.

[1] The abbreviations used are: MPR, cation-independent mannose 6-phosphate receptor; RAP, receptor-associated protein; LRP, low density lipoprotein receptor-related protein; rhIDU, recombinant human α-L-iduronidase; rhGAA, recombinant human acid α-glucosidase; CHOΔL, LRP-null CHO cell line; 4-MUI, 4-methylumbelliferyl-α-L-iduronide; sLRP2, recombinant ligand-binding domain 2 of LRP1; RAP-IDU, fusion of RAP and IDU; RAP-GAA, fusion of RAP and GAA; Bis-7, oligomannose 7 bisphosphate; PBS, phosphate-buffered saline; LDL, low density lipoprotein; LDLR, low density lipoprotein receptor; FBS, fetal bovine serum; BSA, bovine serum albumin; CHO, Chinese hamster ovary; Endo H, endoglycosidase H; FACE, fluorophore-assisted carbohydrate electrophoresis; Bis-Tris, 2-[bis(2-hydroxyethyl)amino]-2-(hydroxymethyl)propane-1,3-diol.

RAP binds to particular pairs of these repeats with dissociation constants in the low nanomolar range (21, 22). Whereas undetectable in circulating plasma, intravenous injection of RAP results in rapid, receptor-mediated uptake into tissues (23, 24).

This report describes fusions between RAP and two human lysosomal enzymes, α-L-iduronidase (IDU) and acid α-glucosidase (GAA). IDU is the deficient enzyme in Hurler/Scheie syndrome; GAA is the deficient enzyme in Pompe syndrome. These fusion proteins have been characterized with respect to enzyme activity, glycosylation, LRP binding, and receptor-dependent uptake into cells. We have determined that the fusions retain the receptor binding ability of RAP as well as the catalytic activity of the lysosomal enzyme. Our evidence supports uptake of the fusions into cells followed by delivery to the lysosome and degradation of the RAP moiety, leaving the lysosomal enzyme cargo intact. This system represents a highly efficient alternative to oligosaccharide receptor-dependent delivery of lysosomal enzymes to the cells of affected patients, and offers the possibility of transport of lysosomal enzymes across endothelial cell layers connected by tight junctions, such as those that make up the blood-brain barrier.

EXPERIMENTAL PROCEDURES

Materials—Human fibroblasts were obtained from the Coriell Cell Repository. Rat C6 glioblastoma cells and mouse C2C12 myoblasts were obtained from the American Type Culture Collection (ATCC). Recombinant human RAP, expressed in bacteria, was purified as previously described (25). Cell lines for the expression of sLRP2 were kindly provided by Professor Anton-Jan van Zonneveld (University of Amsterdam); the receptor fragment was purified as described (27). Human serum and plasma were purchased from Sigma. All chromatography media were from Amersham Biosciences.

Antibodies and Western Blot Analysis—New Zealand White rabbits were immunized with purified preparations of rhIDU, rhGAA, or RAP. Polyclonal antisera were analyzed for antibody titer and antigen specificity. Antibodies were found to be highly specific for their respective antigens.

For Western blotting, proteins were separated by reducing SDS-PAGE, electroblotted to nitrocellulose membranes, and blocked for 1 h at room temperature with blocking buffer containing 2% (w/v) dry milk powder in Tris-buffered saline (20 mM Tris-HCl, 150 mM NaCl, pH 7.5) with 0.05% (v/v) Nonidet P-40. For detection of rhIDU antigen, anti-rhIDU antiserum (BP13, BioMarin) was diluted 25,000-fold into blocking buffer. For detection of GAA antigen, anti-rhGAA antiserum (BP32, BioMarin) was diluted 2,500-fold into blocking buffer. For detection of RAP antigen, purified anti-RAP IgG (BP41/42, BioMarin) was diluted to 0.022 μg/ml into blocking buffer. Bound primary antibodies were detected with affinity purified alkaline phosphatase-conjugated goat secondary antibody (Promega) diluted 5,000-fold in blocking buffer. Blots were developed with Western Blue™ colorimetric substrate (Promega), rinsed with distilled water, and scanned.

Fusion Expression Constructs—The human RAP coding sequence, encompassing amino acids 35–353, was amplified from human liver cDNA using PfuTurbo™ polymerase (Stratagene) and the primers RAPF (5′-GCGATAGGATCCTACTCGCGGGAGAAGAACCAGCCCAAGCCGTCCCCGA-3′) and RAPR (5′-GCGATAAACCGGTTTCTGCCTCGGCGCGAGCTCTGGAGATCCTGCCGGACAGGTCCT-3′). This por tion of the RAP coding sequence includes neither the signal peptide nor the endoplasmic reticulum retention signal (HNEL). The RAP sequence encoded by the amplified fragment was identical to that previously reported (GenBank™ accession NM_002337). The 5′-RAP primer incorporates an in-frame BamHI site at the 5′-end. The 3′-RAP primer adds sequence encoding a six amino acid spacer (AEAETG), which also includes an in-frame AgeI site at the 3′-end. The modified RAP sequence was ligated into an expression vector as an in-frame fusion with either human IDU (amino acids 27–652) or human GAA (amino acids 70–952). Both lysosomal enzyme sequences lacked their signal peptides and, in the case of GAA, the propeptide sequence as well. Both IDU and GAA sequences were modified by PCR to include in-frame 5′-AgeI sites and 3′-XhoI sites. The human IDU sequence was amplified with primers: IDUfuseF, 5′-GCGATAACCGGTGAGGCCCCGCACCTGGTGCATGTGGACGCGGCCCGCGCGCTGTGG-3′; and IDUfuseR, 5′-GCGATACTCGAGTCATGGATTGCCCGGGGATGGGGGCCCTCTTGGCACAGGGACC-3′. The amplified IDU fragment was sequenced and found to be identical to the equivalent portion of the IDU cDNA used to manufacture the rhIDU used in these studies (26). The human GAA sequence was amplified with primers: GAAfuseF, 5′-GCGATAACCGGTGCACACCCCGGCCGTCCCAGAGCAGTGCCCAC-3′; and GAAfuseR, 5′-CTCGAGTCAACACCAGCTGACGAGAAACTGCTCTCCCCATCAACAGC-3′. The amplified GAA fragment was sequenced and found to encode a protein sequence identical to that previously published (GenBank accession NM_0001520). The BamHI-AgeI-digested RAP and AgeI-XhoI-digested IDU or GAA fragments were ligated into a BamHI-XhoI-digested expression vector based upon pcDNA3.1(+) (Invitrogen). The vector was modified to include the rabbit β-actin IVS2, the rat preproinsulin transcript leader sequence, and the first 18 amino acids (signal peptide) of human melanotransferrin. The melanotransferrin signal peptide contained a 3′-BamHI site allowing in-frame fusion to RAP.

Plasmid vectors were linearized with AclI and transfected into an LRP1-null CHO-K1 line (CHOΔL) using Cytofectene™ (Bio-Rad). Transfections were performed exactly as specified by the manufacturer's protocol. Clones were selected by limiting dilution in medium containing 800 μg/ml G418 and screened for expression using fluorescent monosaccharide substrates for the respective lysosomal enzymes. Clones expressing RAP-IDU (CHOΔL-RI7) and RAP-GAA (CHOΔL-RG20) were selected for further studies.

Expression of RAP Fusions—CHOΔL-RI7 and CHOΔL-RG20 were cultured in T-flasks using a protein-free medium (JRH) supplemented with 2.5% fetal bovine serum (FBS). Production was carried out in the absence of serum in pH, oxygen, and temperature-controlled 3L Applikon bioreactors. Cells were grown on Cytopore 1™ microcarrier beads (Amersham Biosciences) for the production phase. Microcarriers were retained during perfusion using an internal settler device. Bioreactor perfusion rates were determined by monitoring residual glucose in the medium.

Purification of RAP Fusions—RAP fusion-containing cell culture media was clarified by passage through Sartopore 1.2-μm depth filters (Sartorius) and then sterilized by sequential passage through 0.45- and 0.2-μm PES membrane filters. The protease inhibitors L-1-tosylamido-2-phenylethyl chloromethyl ketone and phenylmethylsulfonyl fluoride were included in the media prior to filtration to mitigate proteolysis of the RAP portion of the fusions. The sterile, clarified medium containing the RAP-IDU fusion was pH adjusted to 6.5 and then sequentially resolved on Heparin-Sepharose CL-6B, Phenyl-Sepharose HP, and SP-Sepharose Fast Flow. Enzymatically active fractions were pooled, concentrated, and when necessary, diafiltered using a 50-kDa molecular mass cut-off mini-TFF membrane (Vivascience). RAP-GAA was purified with an initial DEAE Fast Flow flow-through step. The fusion was then sequentially resolved on Heparin-Sepharose CL-6B and Phenyl-Sepharose HP. In-process and final eluates were treated as described for RAP-IDU. Both purified RAP fusions were formulated in 10 mM sodium phosphate, pH 5.8, 150 mM NaCl.

Expression and Purification of RhIDU and RhGAA—Human lysosomal α-L-iduronidase and acid α-glucosidase were expressed and purified essentially as previously described (26, 28, 29). The purified enzymes were greater than 95% pure as judged by SDS-PAGE.

Enzyme Activity Assays—Enzyme activities were determined by the hydrolysis of small fluorigenic monosaccharide substrates in a 96-well plate format. Specifically, IDU activity was measured by serially diluting samples in phosphate-buffered saline (PBS), pH 5.8, containing 200 μg/ml BSA. Diluted samples were preincubated at 37 °C for 20 min prior to adding substrate. 4-Methylumbelliferyl-α-L-iduronide (4-MUI, Toronto Research Chemicals) was then added as a 5 mM stock solution in 400 mM sodium formate, 150 mM NaCl, 0.1% Triton X-100. The final 4-MUI concentration was 2.5 mM. Reactions were incubated for 10 min at 37 °C prior to quenching with stop solution at pH 11. Fluorescence was measured with a microplate fluorimeter (Molecular Devices) using an excitation wavelength of 366 nm and an emission wavelength of 446 nm. GAA activity was measured by serially diluting samples in 62 mM sodium citrate, 77 mM sodium phosphate, 0.3 mg/ml BSA, 0.01% sodium azide, pH 4.0. 4-Methylumbelliferyl-α-D-glucoside was diluted from an ethylene glycol monomethyl ether stock solution into the same buffer and added to the diluted samples to a final concentration of 0.6 mM. Reactions were incubated for 30 min at 37 °C before quenching with stop buffer at pH 11. Assay results represent the mean of at least four dilutions giving values in the linear range. All samples were run in duplicate. Standard deviations of assay samples did not exceed 6% of the mean value. One milliunit of enzyme activity is defined as 1 nmol of 4-methylumbelliferone produced per min at 37 °C.

Kinetic Analysis of RhIDU and RAP-IDU—RhIDU and RAP-IDU at final concentrations of 1 nM were incubated at 22 °C for 5 min in PBS,

pH 5.8, containing 200 μg/ml BSA and 0.016, 0.031, 0.063, 0.125, 0.25, 0.5, 1, and 2 mM 4-MUI. Assays were otherwise performed as described above. Results were plotted as milliunits of IDU activity per min for each substrate concentration. Curves were fitted using GraphPad Prism software. Derived V_{max} and K_m values with standard errors are listed in Table I.

Protein Mass Measurements—Protein concentrations were determined using A_{280} values for purified protein preparations and theoretical calculations of extinction coefficients based on amino acid composition. The latter were obtained using ProtParam software.

Degradation of RAP Fusions by Lysosomal Proteases in Vitro—Lysosomal proteases cathepsin B, D, and L (Calbiochem) were reconstituted in 50 mM sodium acetate, pH 5, and stored frozen. For the digests, 1 μg of each fusion protein was incubated with an equimolar mixture of cathepsins, ~80 nM final concentration for each, in 100 mM sodium acetate, 100 mM NaCl, 0.5 mM dithiothreitol, pH 4.5, for 1 h at 37 °C. Reactions were quenched with protease inhibitor mixture (Sigma) followed by the addition of 2% SDS sample loading buffer and heating for 5 min at 95 °C. Samples were resolved on 4–20% gradient Tris-glycine SDS-PAGE gels (Invitrogen) and stained with Coomassie Blue.

Characterization of Oligosaccharides by Fluorophore-assisted Carbohydrate Electrophoresis (FACE)—FACE analysis was performed essentially as described (30, 31). Briefly, proteins (200–400 μg) were denatured and treated with *N*-glycanase (Prozyme) to release *N*-linked oligosaccharides. Isolated oligosaccharides were then fluorescently labeled by reductive amination with 8-aminonaphthalene-1,3,6-trisulfate and resolved on polyacrylamide gels with fluorescence detection. Band identity was inferred by measuring mobility relative to known oligoglucose standards. When necessary, oligosaccharide identities were confirmed by additional FACE analysis after digestion with specific exoglycosidases.

Characterization of Oligosaccharides by Isoelectric Focusing—Purified fusions were treated with *Clostridium perfringens* neuraminidase (Sigma) in 50 mM sodium acetate buffer, pH 5, at 37 °C for 1 h. Treated samples and untreated controls were analyzed by isoelectric focusing (IEF) on pH 3–9 Phastgel™ gradient gels (Amersham Biosciences).

Characterization of Oligosaccharides by Digestion with Endo H and N-Glycanase—Following digestion with cathepsins as described, samples were incubated with Endo H (New England Biolabs) or *N*-glycanase (Prozyme) using the manufacturer's protocols and resolved on 4–20% gradient Tris glycine SDS-PAGE gels with Coomassie Blue staining.

Ligand Blots—Polyvinylidene difluoride membranes (Millipore) were pre-wet in methanol and then equilibrated in PBS (11.9 mM sodium phosphate, 137 mM NaCl, 2.7 mM KCl, pH 7.4). Membranes were then mounted in a Bio-Rad dot blot apparatus. The second ligand-binding domain of LRP1 (sLRP2, 1 μg/well) was applied to the membrane by vacuum filtration. The membrane was then cut into sections that were placed in separate wells of a 24-well plate. Membranes were blocked in Tris-buffered saline (20 mM Tris-HCl, pH 7.4, 150 mM NaCl) with 5 mM $CaCl_2$ and 3% nonfat dry milk for 30 min. Test proteins were incubated with each membrane spot for 2 h at room temperature. Individual spots were washed twice for 5 min with blocking buffer and then incubated with anti-RAP or anti-IDU antibodies in the same buffer for 1 h at room temperature to detect binding of the ligand to sLRP2.

Stability of RAP Fusions in Serum and Plasma—RAP-IDU was diluted to 150 μg/ml in human serum and plasma, both adjusted to pH 7.4 with 0.5 M sodium phosphate, pH 6.8. Diluted samples were assayed for volumetric IDU activity (milliunits/ml) and integrity by Western blotting prior to incubation in a 37 °C dry incubator for 30 min, 1 h, 2 h, 4 h, and 7 h. Following incubation, samples were assayed again for both volumetric IDU activity and integrity on Western blots. For comparison, RAP-IDU was incubated for similar intervals in the final formulation buffer, 10 mM sodium phosphate, pH 5.8, 150 mM NaCl.

Uptake of RAP Fusions into Cell Lines—Fibroblasts and myoblasts were grown in Dulbecco's modified Eagle's medium supplemented with 10% FBS; C6 glioma cells were grown in Ham's F-10 supplemented with 15% horse serum in addition to 2.5% FBS. For the determination of the half-life of GAA in fibroblasts, the FBS used in the cell culture medium was treated to inactivate endogenous GAA activity by adjusting to pH 10 with NaOH, incubating for 30 min at 37 °C, and then readjusting to pH 7.4 with HCl. For each uptake experiment, appropriate test proteins were diluted into serum-free growth media containing 20 mM HEPES, pH 7.0, and 0.5 mg/ml BSA and incubated with cells, in duplicate, for various intervals up to 2 h. Uptake experiments were performed in 12-well tissue culture plates. Test protein concentrations were determined from A_{280} measurements and theoretical extinction coefficients based on amino acid composition. Following incubation, cells were rinsed with PBS, and trypsinized. Cell pellets were collected by low-speed centrifugation, washed with cold PBS, and lysed by freezing at −80 °C in the presence of 0.1% Triton X-100. Lysates were clarified by centrifugation. The soluble lysate fractions were assayed in duplicate for enzyme activity as described and for total protein using the Pierce bicinchonic acid (BCA) method. In some cases, lysate samples were resolved on SDS-PAGE gels and analyzed by Western blotting as previously described.

Uptake of RAP-IDU into Fibroblasts in the Presence of Serum—Experiments were done exactly as described above except that the uptake medium contained 50% fetal bovine serum (Irvine Scientific catalog number 3000A).

Uptake of RAP Fusions into Cells Expressing Specific LRP Receptors—RAP-GAA was labeled with $Na^{125}I$ using Iodogen beads (Pierce). Unincorporated label was removed by gel filtration on PD-10 columns (Amersham Biosciences). An aliquot of the labeled fusion was trichloroacetic acid precipitated and specific activity was calculated. CHO LRP-null cells stably expressing different LDLR family receptors or Brown Norway rat yolk sac cells expressing megalin (100,000 cells/well) were seeded in 24-well plates 1 day prior to the experiment. Cells were then incubated with ^{125}I-RAP-GAA (5 nM) for 4 h at 37 °C in minimal Dulbecco's modified Eagle's medium containing 5 mM $CaCl_2$ and 6 mg/ml BSA. Each cell type was tested in triplicate with and without 500 nM unlabeled RAP. After incubation, conditioned medium was removed and proteins were precipitated with 20% trichloroacetic acid. Remaining soluble counts were measured in a γ-counter. Cells were washed with PBS, lysed with 1 N NaOH, and total protein determined by the Bio-Rad Bradford assay (12, 32).

Prevention of Glycosaminoglycan Accumulation in Hurler Fibroblasts by Incubation with IDU or RAP-IDU—Human GM1391 Hurler fibroblasts were grown in Dulbecco's modified Eagle's medium containing 10% fetal bovine serum and 2 mM glutamine. Four days prior to the experiment, cells were seeded in 6-well plates at 250,000 cells per well. On the day of the experiment, cells were fed with sulfate-free medium (Irvine Scientific), 15% fetal bovine serum, 5 mM $CaCl_2$ for 1 h and then the same medium was supplemented to 4 μCi/ml with [^{35}S]sodium sulfate and 5 nM of either RAP-IDU or rhIDU alone. Cells were incubated in this medium for 48 h at 37 °C in a humidified cell culture incubator with 5% CO_2, 95% air. Cell layers were rinsed three times with PBS before and after trypsinization. Pellets were lysed in 0.5 N NaOH and neutralized with 1 M HCl. Protein concentrations were determined by Bio-Rad Bradford assay in 96-well plates. Radioactivity in the lysates was counted in Beckman ReadyCaps™.

RESULTS

Expression of Fusion Proteins—RAP fusions were configured such that the RAP coding sequence was located N terminal to the lysosomal enzyme coding sequence. The order of the sequences was based on previously published studies demonstrating that GST-RAP fusions, in which RAP is located C-terminal to GST, had up to 10-fold lower affinity for LRP than RAP alone (23).[2] A CHO-K1 mutant (CHOΔL) was chosen for production of the RAP fusions (33). CHOΔL does not express any LRP receptors, preventing reuptake and degradation of secreted protein by the overexpressing cell line. CHOΔL does express LDLR, but reuptake of fusion by this receptor is expected to be minimal because of its low affinity for RAP. Fusions between RAP and both IDU (RAP-IDU) and GAA (RAP-GAA) were expressed in this system. Clones for each fusion were selected based on enzyme activity in the cell culture medium and scaled-up for production in bioreactors. Volumetric productivity values were calculated from activity concentrations (units/liter) and the specific activities (units/mg) of purified rhIDU or rhGAA. Calculated in this way, the average daily reactor productivities were 1–2 mg/liter/day for RAP-IDU and 10–15 mg/liter/day for RAP-GAA.

Purification and Characterization of Fusions—Fusions were purified to >95% using conventional resins (Fig. 1, *A* and *B*, *lane 1*). Anti-RAP antibodies (Fig. 1, *A* and *B*, *lane 2*) and either

[2] We have subsequently observed that reversing the order of RAP and IDU in the fusion blocks the ability of RAP to bind to LRP on filters, data not shown.

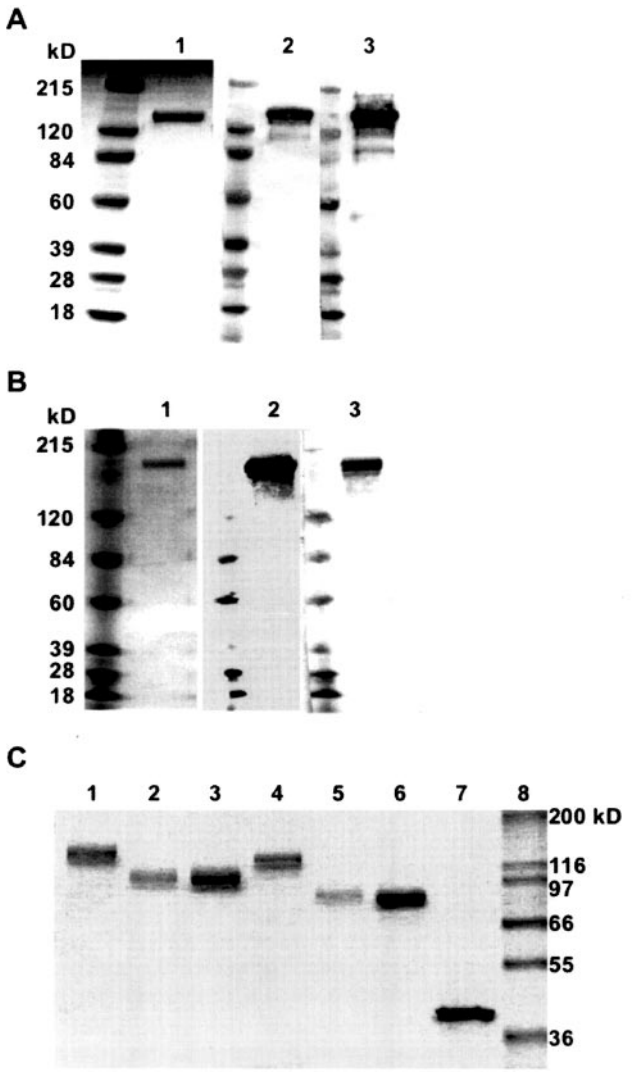

FIG. 1. **Gel and blot analysis of intact and proteolyzed RAP fusions.** Intact RAP fusions: *A*, RAP-IDU; and *B*, RAP-GAA. Purified fusions (3 μg for Coomassie Blue staining, 0.5 μg for Western blotting) were resolved on 4–12% gradient Bis-Tris SDS-PAGE gels under reducing conditions. Western blots were performed as described under "Experimental Procedures." A molecular weight marker lane is located to the *left* of each sample lane. *Lane 1*, Coomassie Blue staining; *lane 2*, anti-RAP antibody; *lane 3*, anti-IDU (*A*) or anti-GAA (*B*) antibody. *C*, *in vitro* proteolyzed RAP fusions. Fusions (1 μg) were treated with a mixture of cathepsins, resolved on 4–20% gradient Tris glycine SDS-PAGE gels under reducing conditions and stained with Coomassie Blue. *Lane 1*, undigested RAP-GAA fusion; *lane 2*, proteolyzed RAP-GAA fusion; *lane 3*, rhGAA; *lane 4*, undigested RAP-IDU fusion; *lane 5*, proteolyzed RAP-IDU fusion; *lane 6*, rhIDU; *lane 7*, RAP; *lane 8*, molecular mass markers.

anti-IDU or anti-GAA antibodies (Fig. 1, *A* and *B*, *lane 3*) co-stained bands consistent with the molecular weights of each fusion on Western blots of conditioned cell culture medium. Although stable in conditioned medium, the fusions were observed to be sensitive to proteolytic cleavage events during purification. The proteolysis resulted in the removal of RAP from the N terminus of both fusion proteins. Proteolysis was mitigated by addition of protease inhibitors to the conditioned medium prior to purification.

Molar specific activities of the purified fusions were calculated by dividing enzyme activity concentrations (units/ml) by protein concentrations (nmol/ml) of the fusion. Fusion concentrations were calculated from A_{280} measurements and theoretical extinction coefficients (Table I). RAP-IDU had a molar specific activity of 5.7 units/nmol, whereas rhIDU had a molar specific activity of 12.5 units/nmol. The substantial difference in molar specific activities for RAP-IDU and rhIDU suggests that RAP interferes in some way with the catalytic activity of IDU within the context of the fusion. The diminished activity of the fusion could involve restriction of access to the active site, alterations in the folding of IDU, or other conformational constraints that affect protein motions involved in catalysis. To gain more insight into the catalytic differences between rhIDU and RAP-IDU, kinetic parameters for cleavage of 4-MUI were measured. Whereas the K_m values for the two proteins were indistinguishable, the V_{max} for rhIDU exceeded that of RAP-IDU by 25% (Table I). This difference is consistent with some constraint being imposed on the motion of IDU within the context of the fusion rather than restricted access to the active site. RAP-GAA and rhGAA were found to have nearly identical molar specific activities. Therefore, the effect of fusing a protein to RAP will likely depend on the specific protein in question.

Digestion of RAP Fusions with Lysosomal Proteases—To simulate how the fusions might behave in the lysosome, we incubated RAP-IDU and RAP-GAA with a mixture of cathepsin D, B, and L at pH 4.5 at 37 °C for 1 h. Digested proteins were analyzed by SDS-PAGE. RAP was degraded under these conditions, leaving the lysosomal enzyme intact (Fig. 1*C*, *lanes 2* and *5*). The major band remaining for each of the two fusions was slightly larger than rhIDU and rhGAA. The additional mass may be an indication that some RAP or linker sequence remains after treatment.[3] GAA activity per volume of digest was not significantly affected by *in vitro* proteolysis (data not shown). This result is consistent with the similar molar specific activities of RAP-GAA and rhGAA. IDU activity per volume of digest increased by 26% after *in vitro* proteolysis of the fusion, suggesting a partial restoration of the enzymatic activity of the released IDU moiety compared with rhIDU. The specific activity of fusion-derived IDU after delivery to the lysosome was not determined.

Characterization of RAP Fusion Oligosaccharides—Given the important role that oligosaccharide receptors play in the uptake of lysosomal enzymes *in vivo*, we sought to determine what types of oligosaccharides were present on the RAP fusions. First, purified fusions were subjected to FACE analysis to measure levels of phosphorylated oligosaccharides relative to the native lysosomal enzymes (Fig. 2*A*). Phosphorylated oligosaccharides are readily identified by their characteristic mobilities on FACE gels. Both rhIDU and rhGAA possessed significant amounts of bis-phosphorylated oligomannose 7 (Bis-7), a structure that is bound tightly by the MPR (2) (Fig. 2*A*, *lanes 2* and *5*, *arrow*). Each oligosaccharide band was quantitated by fluorescence intensity. Bis-7 accounted for 30 and 20% of all oligosaccharides on rhIDU and rhGAA, respectively. In both cases, these percentages are consistent with 1–2 molecules of Bis-7 for each molecule of enzyme. Whereas the rhIDU and RAP-IDU oligosaccharide profiles were otherwise similar, the fusion carried 60% less Bis-7 compared with the enzyme alone (Fig. 2*A*, *lane 6*). This value equates to roughly one molecule of Bis-7 for every three molecules of RAP-IDU fusion. The rhGAA and RAP-GAA oligosaccharide profiles were also similar (Fig. 2*A*, *lanes 2* and *3*), but, in contrast to RAP-IDU, no phosphorylated oligosaccharides were found in significant amounts on the RAP-GAA fusion.

To test for complex oligosaccharides terminating in sialic acid, we next subjected the RAP-GAA fusion to IEF analysis after treatment with neuraminidase (Fig. 2*B*). A shift of the

[3] N-terminal sequencing and peptide mapping indicate that cleavage occurs at multiple sites within the last 20 amino acids of RAP and the linker sequence (data not shown).

TABLE I
Physical parameters of RAP fusion proteins

	rhIDU	RAP-IDU	rhGAA	RAP-GAA
Amino acids	627	952	883	1,208
Apparent M_r (SDS-PAGE)	83,000	125,000	110,000	150,000
Theoretical protein M_r	70,000	108,000	98,000	136,000
Theoretical ε M^{-1} cm^{-1}	118,280	154,410	159,890	196,020
Activity concentration	104 units/ml	7.4 units/ml	6.2 units/ml	5.1 units/ml
Protein concentration	8.3 nmol/ml	1.3 nmol/ml	21 nmol/ml	16 nmol/ml
Molar specific activity	12.5 units/nmol	5.7 units/nmol	0.29 units/nmol	0.32 units/nmol
K_m (4-MUI)	0.3 ± 0.02 mM	0.3 ± 0.03 mM	NA[a]	NA
V_{max} (units at 24 °C)	1.65 ± 0.03	1.22 ± 04	NA	NA
Bis-7	+++	+	+++	−

[a] NA, not applicable.

fusion to more basic isoelectric points provided evidence that RAP-GAA contained sialylated complex oligosaccharide (Fig. 2*B*, compare *lanes 3* and *4*). The positive control, rhIDU, underwent a similar shift upon treatment with neuraminidase (Fig. 2*B*, compare *lanes 1* and *2*).

The large size of the fusions made it difficult to analyze oligosaccharide mass and content by digestion with glycosidases. To reduce the size of the protein component, samples of RAP-IDU and RAP-GAA were digested with cathepsins. Proteolyzed fusions were then further digested with Endo H or *N*-glycanase to release high-mannose oligosaccharides and total oligosaccharides, respectively. This experiment does not address the oligosaccharide content of the RAP portion of the fusion because RAP is lost upon cathepsin proteolysis. RAP has one glycosylation site. Endo H digestion of proteolyzed RAP-GAA had little effect on band mobility, indicating minimal high-mannose or hybrid oligosaccharides on the GAA part of the fusion (Fig. 2*C*, compare *lanes 3* and *4*). Digestion of proteolyzed RAP-GAA with *N*-glycanase resulted in a band shift of 17 kDa. This result is consistent with the isoelectric focusing experiment in that both demonstrate high levels of complex oligosaccharides on the RAP-GAA fusion. In contrast with RAP-GAA, Endo H digestion of proteolyzed RAP-IDU resulted in a significant band shift, consistent with the presence of high-mannose or hybrid oligosaccharides on fusion-derived IDU (Fig. 2*C*, compare *lanes 7* and *8*).[4] By mass, the loss upon digestion of IDU with Endo H accounted for the majority of the total loss observed upon digestion with *N*-glycanase (Fig. 2*C*, *lane 9*).

Ligand Blotting—We next sought to determine whether the RAP portion of the RAP-IDU fusion was able to bind to receptor. To this end, recombinant sLRP2, the entire second ligand-binding domain of human LRP1, was spotted onto nylon membrane filters (Fig. 3). After blocking, individual filters were incubated with RAP (*column B*), RAP-IDU (*column C*), or rhIDU (*column D*) in binding buffer. Filters were washed and probed with anti-RAP (*row 1*) or anti-IDU antibodies (*row 2*). Judging by signal intensity, RAP-IDU bound to the receptor fragment as well as RAP alone under these conditions (*columns B* and *C*, *row 1*). Binding of RAP and RAP-IDU could be blocked with excess cold RAP (*column C*, *row 3*). Recombinant human IDU did not bind to sLRP2 (*column D*). These results demonstrate that the RAP moiety within the RAP-IDU fusion retains the ability to specifically bind to LRP.

Uptake of RAP Fusions into Patient Fibroblasts—To test whether RAP fusions could be taken up into cells in culture, RAP-IDU, RAP-GAA, rhIDU, or rhGAA were added to primary human fibroblasts isolated from either Hurler (IDU-deficient, GM1391) or Pompe (GAA-deficient, GM244) patients. Test protein concentrations for the uptake experiments were calculated from A_{280} measurements and theoretical extinction coefficients. Following an interval of 1–2 h to allow for uptake, cells were harvested, lysed, and assayed for lysosomal enzyme activity. Uptake signal for RAP-IDU is reported in units of fluorescent substrate cleaved per volume of lysate, uptake signal for RAP-GAA is reported in units of relative fluorescence units per volume of lysate. Identical numbers of cells were used in each well and normalizing the activity data to total protein in each sample did not change the results. Curves were fitted to hyperbolic functions and uptake parameters were derived using GraFit software (Erithacus). The hyperbolic asymptote value is defined here as the maximum uptake capacity. The concentration of fusion or enzyme giving half-maximal uptake is defined, as it has been previously, as K_{uptake} (34).

Fibroblasts in culture were found to take up significantly more RAP fusion than enzyme alone (Fig. 4, *A* and *B*, and Table II). This difference became more pronounced at higher concentrations of fusion and enzyme. In particular, the maximum uptake capacity for the fusion in Hurler fibroblasts exceeded that of the free enzyme by 43-fold in the case of RAP-IDU despite a 25-fold K_{uptake} advantage for the rhIDU. Because the specific activity of the RAP-IDU fusion is about half that of rhIDU, uptake of fusion may be underestimated in this experiment. The maximum uptake capacity for RAP-GAA in Pompe fibroblasts exceeded that of rhGAA by 70-fold despite a 25-fold K_{uptake} advantage for rhGAA (Fig. 4*B* and Table II).

Inhibitors of LRP (RAP) and MPR (mannose 6-phosphate) receptors were included in the culture media to determine whether RAP-IDU and RAP-GAA uptake into fibroblasts was receptor-specific. Excess RAP significantly inhibited uptake of RAP-IDU and RAP-GAA in fibroblasts (Fig. 4, *panels C* and *D*). Conversely, excess mannose 6-phosphate had minimal effects on the uptake of RAP-GAA into the same cells (Fig. 4*D*).

Similar uptake and inhibition experiments were then carried out using a brain cell line, rat C6 glioma cells (Fig. 4*E*) and a muscle cell line, mouse C2C12 myoblasts (Fig. 4*F*). At 5 nM concentrations, the uptake of RAP-IDU into C6 glioma cells was as efficient as rhIDU (Table II); at 50 nM concentrations, uptake of RAP-IDU exceeds that of rhIDU by 1.8-fold. At 5 nM concentrations, uptake of RAP-GAA was 18-fold more efficient than rhGAA in C2C12 myoblasts. As was the case in the fibroblasts, uptake of the RAP fusions into either cell line was inhibited by RAP but not by mannose 6-phosphate. These results show that fusions were efficiently taken up by cells in culture, that uptake occurred in a receptor-dependent manner, and that the relative uptake of fusions and lysosomal enzymes differed significantly between different types of cells.

Uptake of RAP-IDU into Fibroblasts in the Presence of Serum—The RAP portion of the RAP fusions must be able to compete with high concentrations of other LDLR family ligands in the blood, including activated α_2-macroglobulin and a variety of lipoproteins. To test the effect that this competition might have on the uptake of RAP-IDU into fibroblasts, uptake

[4] Note that the RAP-IDU sample used for this experiment was already partly proteolyzed during purification.

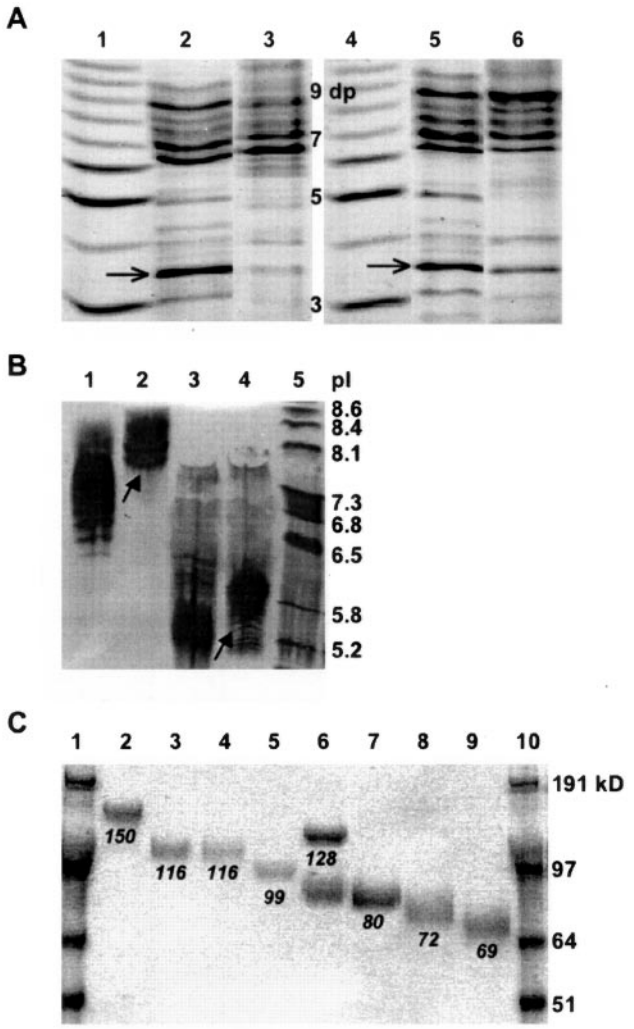

FIG. 2. **Analysis of RAP fusion oligosaccharides.** *A*, FACE of GAA, RAP-GAA, rhIDU, and RAP-IDU: *N*-linked oligosaccharides were released from proteins (~200 μg), fluorescently labeled at the reducing terminus, and electrophoresed as described under "Experimental Procedures." Fluorescent bands were analyzed on a FACE imager system. Band intensity is proportional to the molar amount of particular oligosaccharides present. *Lanes 1* and *4*, oligoglucose ladder calibrated in degree of polymerization (*dp*) units; *lane 2*, rhGAA; *lane 3*, RAP-GAA; *lane 5*, rhIDU; *lane 6*, RAP-IDU. The prominent band near the bottom of *lanes 2* and *5*, marked by the *arrow*, is Bis-7. *B*, isoelectric focusing analysis of complex oligosaccharides on RAP-GAA and rhIDU. Proteins (0.25 μg) were treated with *C. perfringens* neuraminidase, resolved on PhastGels, and silver stained as described under "Experimental Procedures." *Lane 1*, untreated rhIDU (positive control); *lane 2*, rhIDU treated with neuraminidase; *lane 3*, untreated RAP-GAA; *lane 4*, RAP-GAA treated with neuraminidase; *lane 5*, pI standards. *Arrows* indicate a shift to more basic pI after cleavage of terminal sialic acid. *C*, endo H and *N*-glycanase digestion of proteolyzed RAP-GAA and RAP-IDU. Fusions (1 μg) were proteolyzed with a mixture of cathepsins, treated with Endo H or *N*-glycanase, resolved on SDS-PAGE gels, and stained with Coomassie Blue. *Lanes 1* and *10*, molecular weight standards. *Lane 2*, RAP-GAA; *lane 3*, proteolyzed RAP-GAA; *lane 4*, proteolyzed, endo H-digested RAP-GAA; *lane 5*, proteolyzed, *N*-glycanase-digested RAP-GAA; *lane 6*, RAP-IDU; *lane 7*, proteolyzed RAP-IDU; *lane 8*, proteolyzed endo H-digested RAP-IDU; *lane 9*, proteolyzed *N*-glycanase-digested RAP-IDU. Interpolated molecular weights are printed in *italics* under each band.

experiments were carried out in the presence of 50% fetal bovine serum. We observed a modest serum-dependent diminution of uptake at each of three fusion concentrations tested (Fig. 5, A). In particular, the presence of 50% serum in the medium inhibited uptake by 31, 24, and 5% relative to the no

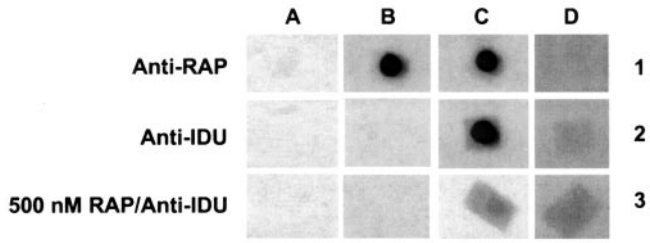

FIG. 3. **Ligand blotting with RAP-IDU.** The second ligand-binding domain of LRP1 (sLRP2, 1 μg) was blotted to nylon membranes and probed with test proteins at a concentration of 5 nM in the presence or absence of 500 nM RAP. Bound proteins were detected by Western blotting with the indicated antibodies as described under "Experimental Procedures." Test proteins were: *column A*, buffer alone; *column B*, RAP; *column C*, RAP-IDU; *column D*, rhIDU.

serum control at RAP-IDU concentrations of 4, 20, and 100 nM, respectively.

Stability of RAP-IDU in Human Serum and Plasma—After injection into the bloodstream, RAP fusions must be stable for an interval sufficient to permit effective tissue distribution and uptake. We sought to gain some measure of the stability of RAP-IDU in blood by diluting the RAP-IDU fusion into human serum or human plasma and incubating at 37 °C. After incubation, samples were assayed for IDU activity and for fusion integrity by Western blotting. We observed that RAP-IDU enzymatic activity did not change significantly over the course of 7 h at 37 °C in either serum or plasma (Fig. 5*B*, *graph*). Similarly, neither anti-IDU Western blots nor anti-RAP Western blots (not shown) demonstrated any changes in the integrity of the fusion upon incubation with serum or plasma (Fig. 5*B*, *inset*, compare *lanes 1* and *2* (buffer) to *lanes 3* and *4* (serum and plasma)). By both measures of stability, RAP-IDU was at least as stable in serum or plasma as it was in buffer alone.

Uptake of RAP-GAA by Different LRP Receptors—We next sought to determine whether fusion uptake could be mediated by specific LDLR family receptors. RAP-GAA was radioiodinated and incubated with a panel of recombinant CHOΔL lines expressing different LDLR family members. Brown Norway rat yolk sac cells were used as the test line for megalin. LRP1 and LRP1B were represented by mini-receptors comprising roughly the C-terminal third of the full-length proteins, which includes the fourth ligand-binding domain, capable of mediating high affinity binding of RAP. Additionally, these mini-receptors possess intact cytoplasmic tails and have been previously shown to faithfully reproduce the trafficking behavior of the full-length receptors (12, 24). Uptake of the fusion was determined by measuring the appearance of soluble counts in the cell culture medium. Soluble counts have previously been demonstrated to reflect uptake, lysosomal delivery, degradation, and release of labeled amino acids from the cells (35). LDLR receptor family-specific uptake was calculated by subtracting the signal obtained in the presence of excess cold RAP competitor (Fig. 6). At a 5 nM concentration, RAP-GAA was specifically taken up and degraded by cells expressing megalin, LRP1, LRP1B, VLDLR, and apoER2 but not LDLR or cells containing empty vector. As LDLR binds to RAP with significantly lower affinity ($K_d \approx 200$ nM (36)) when compared with other members of the LDLR family, this outcome is expected. This experiment confirms that the binding behavior of RAP is predictive of the binding behavior of RAP fusions. Similarly, RAP-inhibitable production of soluble counts indicates that RAP-GAA is endocytosed and lysosomally targeted by the different LRP receptors.

Intracellular Half-life of RAP-GAA—To test the stability of RAP-delivered lysosomal enzyme in the lysosome, we incubated RAP-GAA or rhGAA with Pompe patient fibroblasts (GM244) in multiwell plates for 24 h, transferred them to

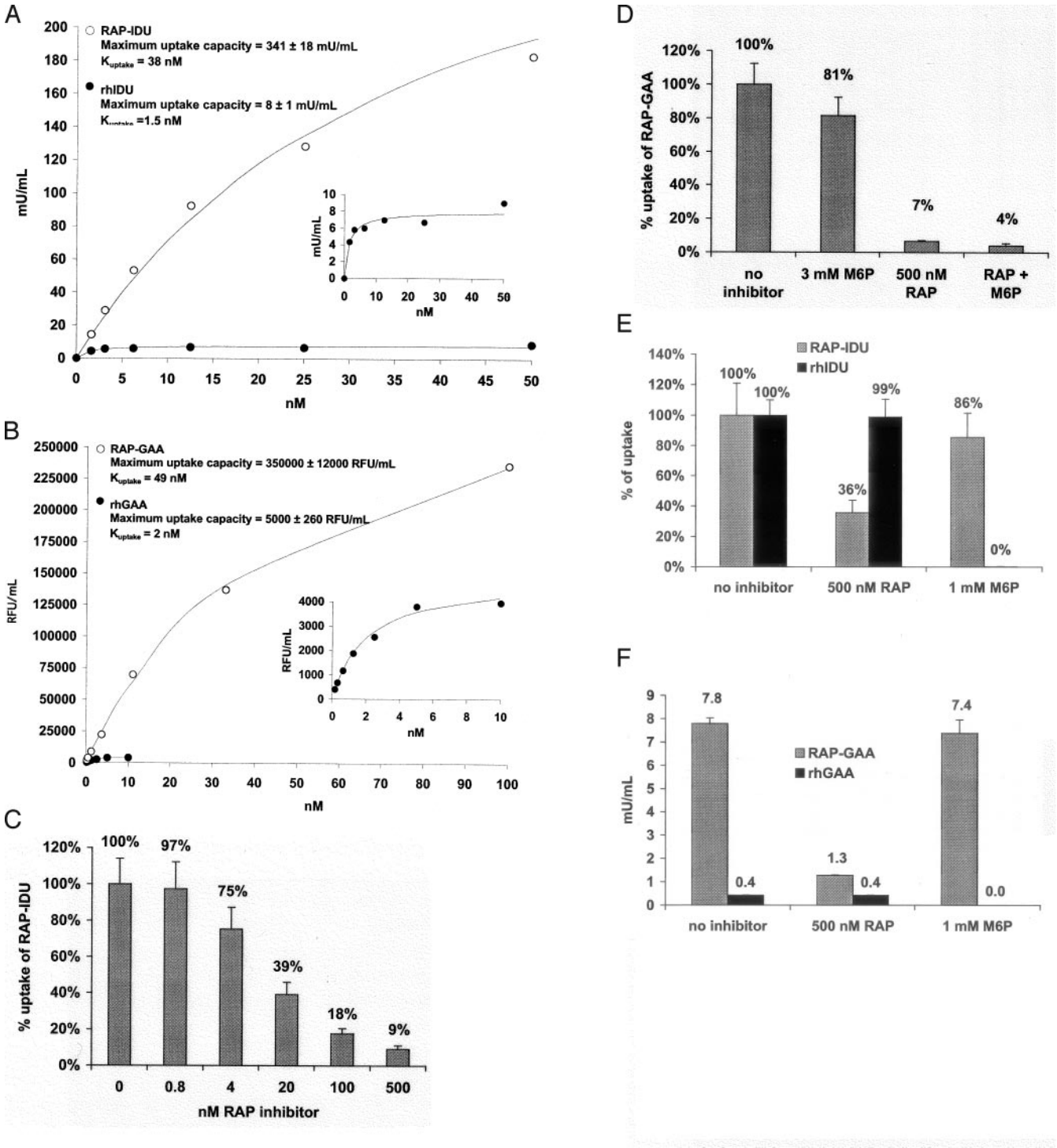

FIG. 4. **Receptor-specific uptake of RAP fusions into cells.** For *A–F*, test proteins were added to duplicate wells of 12-well plates containing the specified cells and incubated for 2 h at 37 °C and 5% CO_2, 95% air in a humidified cell culture incubator. After washing with PBS, cells were lysed and uptake was measured by enzymatic assay as described under "Experimental Procedures." *A*, uptake of RAP-IDU and rhIDU into GM1391 fibroblasts. Different concentrations of RAP-IDU are shown on the *x* axis. Curves were fitted and constants derived as described under "Experimental Procedures." Mean ± S.E. for the derived values are shown. *y* axis units are milliunits of IDU activity per ml of clarified cell lysate. Standard deviations (not shown) for each data point were derived from duplicate well samples. Standard deviations averaged 10% of the mean value and did not exceed 30% of the mean value in any case. *Inset*, plot of rhIDU data alone. *B*, uptake of RAP-GAA and rhGAA into GM244 fibroblasts: *y* axis units are blank-corrected relative fluorescent units of GAA activity per ml of clarified cell lysate. Standard deviations (not shown) for each data point were derived from duplicate well samples. Standard deviations averaged 5% of the mean value and did not exceed 10% of the mean value in any case. *Inset*, plot of rhGAA data alone. For *C–F*, uptake was measured in milliunits of IDU or GAA per ml of clarified cell lysate. Mean ± S.D. of duplicate samples are shown. *C*, inhibition of RAP-IDU uptake into GM1391 fibroblasts by RAP. RAP-IDU was used at a concentration of 3 nM. Uptake at different RAP concentrations (*x* axis) is presented as a percentage of the uptake in the absence of RAP. *D*, inhibition of RAP-GAA uptake into GM244 fibroblasts by RAP. RAP-GAA was used at a concentration of 5 nM. Uptake at the specified concentrations of inhibitors is reported as percentage of the uptake in the absence of inhibitors. *E*, inhibition of RAP-IDU (12.5 nM) and rhIDU (1.6 nM) uptake into C6 glioma cells. Uptake at the specified concentrations of inhibitors is reported as percentage of the uptake in the absence of inhibitors. *F*, inhibition of RAP-GAA uptake and rhGAA uptake into C2C12 myoblasts: RAP-GAA and rhGAA were both at 5 nM. Uptake at the specified concentrations of inhibitors is reported in milliunits of GAA activity per ml of lysate.

TABLE II
Ratios of fusion to enzyme uptake at equimolar concentrations in different cell lines

Fusion	Enzyme	Cell type	Uptake ratio (fusion/enzyme)			
			5 nM	50 nM	Saturation	K_{uptake}
RAP-IDU	rhIDU	Fibroblast	7	27	43	25
RAP-GAA	rhGAA	Fibroblast	9	37	70	25
RAP-IDU	rhIDU	C6 glioma	1	1.8		
RAP-GAA	rhGAA	C2C12 myoblast	19			

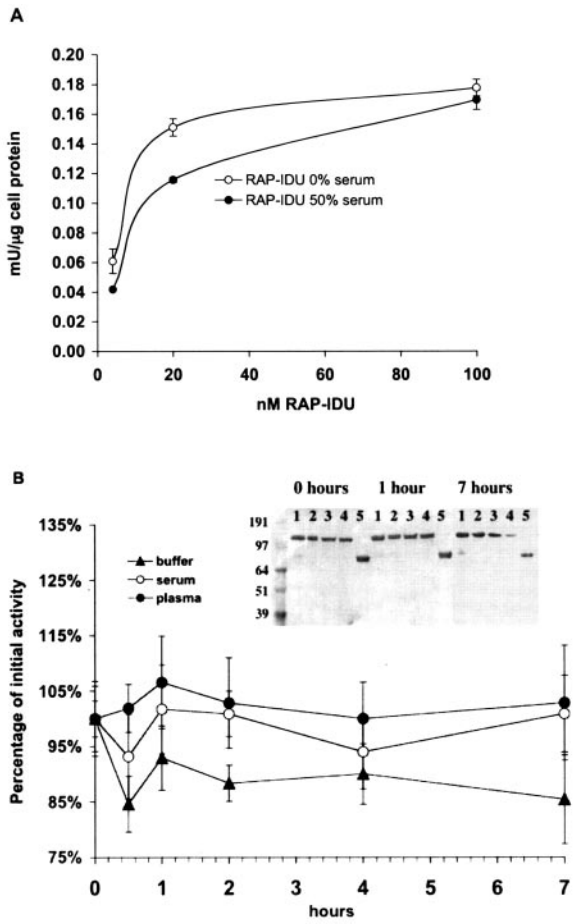

FIG. 5. **Uptake of RAP-IDU in the presence of serum and stability of RAP-IDU in serum and plasma.** *A*, uptake of RAP-IDU into GM1391 fibroblasts in the presence of serum. RAP-IDU at the indicated concentrations was added to duplicate wells in 12-well plates containing fibroblasts. Incubations were carried out for 2 h in the presence or absence of 50% fetal bovine serum. After washing, fibroblasts were lysed and uptake was measured by enzymatic assay. Values are presented as milliunits of IDU activity per μg of total cell protein in clarified cell lysates. Mean ± S.D. of the duplicate well samples are shown. *B*, stability of RAP-IDU in human serum and plasma at 37 °C. RAP-IDU was diluted to 150 μg/ml in PBS, pH 6.5, human serum, or human plasma at pH 7.4. Samples were incubated at 37 °C for 0, 0.5, 1, 2, 4, and 7 h and then assayed for IDU activity in triplicate as described under "Experimental Procedures." Activity remaining after a given interval of incubation is reported as a percentage of the activity at time 0. Mean ± S.D. of the triplicate enzymatic assay samples are shown. *Inset*, Western blot analysis of RAP-IDU stability in human serum and plasma. RAP-IDU was diluted to 150 μg/ml in PBS, pH 6.5, the same buffer at pH 7.4, and human serum or human plasma at pH 7.4, prior to incubation at 37 °C for 0, 1, and 7 h. After incubation, samples were resolved on 4–12% Bis-Tris SDS-PAGE gels. Anti-IDU Western blots were then prepared as described under "Experimental Procedures." *Lane 1*, RAP-IDU in PBS, pH 6.5; *lane 2*, RAP-IDU in PBS, pH 7.4; *lane 3*, RAP-IDU in human serum; *lane 4*, RAP-IDU in human plasma; *lane 5,* rhIDU control.

growth medium lacking the test proteins, and then harvested the cells over a period of 2 weeks. Cell lysates were then assayed for GAA activity. Fusion-derived GAA and rhGAA had

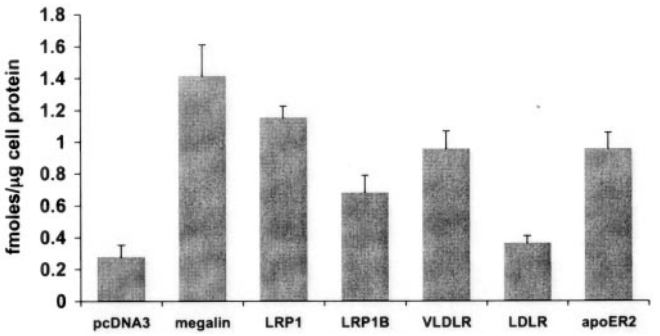

FIG. 6. **RAP-GAA uptake mediated by different LDLR family receptors.** RAP-GAA was labeled with ^{125}I using Iodobeads (Pierce). Unincorporated label was removed by gel filtration on PD-10 columns (Amersham Biosciences). An aliquot of the labeled fusion was trichloroacetic acid precipitated and specific activity was calculated. ^{125}I-RAP-GAA (5 nM) was incubated with CHO LRP-null cells stably expression different members of the LDLR family, or Brown Norway rat yolk sac cells expressing megalin, for 4 h at 37 °C in a humidified cell culture incubator. Uptake and degradation were measured as soluble counts for each sample normalized to total protein from lysed cells of the same sample. Values shown represent the difference in the presence and absence of excess unlabeled RAP (receptor-specific uptake). Mean ± S.D. of the triplicate samples are shown. *y* axis units are femtomoles of solubilized ^{125}I/μg of total protein.

nearly identical intracellular half-lives of ~12 and 10 days, respectively (Fig. 7). Because GAA has a half-life at neutral pH that is measured in hours (data not shown), the nearly identical, multiday half-lives of rhGAA and fusion-derived GAA imply delivery of both to an acidic compartment after endocytosis, most likely the lysosome. Delivery of phosphorylated rhGAA to the lysosome is well documented in the literature and is the basis for ERT with rhGAA (37, 38). Any changes imposed upon GAA as a result of fusion to RAP do not seem to affect the stability of the enzyme in the lysosome. Given the stability of GAA and fusion-derived GAA after uptake and the instability of RAP in the presence of lysosomal enzymes, it is likely that the soluble counts generated after incubation of radiolabeled RAP-GAA with cells (Fig. 6) result from degradation of the RAP portion of the fusion after delivery to the lysosome.

Clearance of Lysosomal Storage with RAP-IDU—Given the attenuated enzymatic activity of fusion-derived IDU *in vitro*, experiments were done to determine whether RAP-IDU could prevent the accumulation of glycosaminoglycan in patient fibroblasts. Hurler fibroblasts were grown in sulfate-free medium in the presence of [^{35}S]sulfate (39). RAP-IDU, rhIDU, or buffer were included in the growth medium at a concentration of 5 nM. Cells were lysed and stored ^{35}S-glycosaminoglycan was measured 48 h later. Radioactivity in the cell lysates was normalized to total protein concentration in the same lysates (Fig. 8). Total radioactivity per sample ranged from 4,000 to 20,000 cpm; total protein concentrations did not vary significantly between samples. Both RAP-IDU and rhIDU prevented ^{35}S-GAG storage to the same extent, indicating that fusion-derived IDU is competent to digest the natural substrate.

DISCUSSION

We have produced and characterized fusions between RAP and two lysosomal enzymes, IDU and GAA. The fusions re-

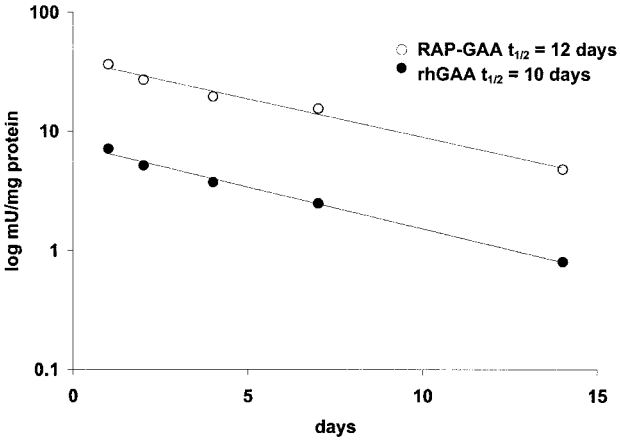

FIG. 7. **Intracellular half-life of RAP-GAA and rhGAA in GM244 fibroblasts.** Fibroblasts were seeded in Dulbecco's modified Eagle's medium with 2 mM glutamine and 10% FBS in 6-well plates. On the day of the experiment, cells were fed with the same medium except that GAA-inactivated FBS was used. RhGAA and RAP-GAA were added to a concentration of 5 nM in duplicate wells of fibroblasts and incubated for 22 h. Medium was exchanged, the cells were rinsed with PBS and then allowed to grow for additional periods from 2 to 14 days. Cells were rinsed with PBS, trypsinized, pelleted, rinsed again, and lysed in PBS, pH 5.8, containing 0.1% Triton X-100 by three cycles of freeze/thaw. Lysates were clarified by centrifugation and assayed for GAA activity as described under "Experimental Procedures." Total protein was measured with the Pierce BCA method. Mean values from the duplicate samples are plotted, standard deviations were in all cases less than 10% of the mean value. Curves were fitted and half-lives calculated using GraFit software.

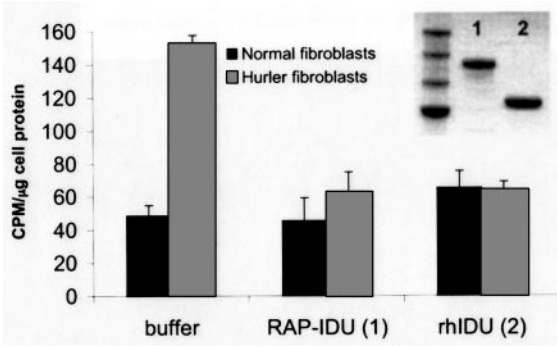

FIG. 8. **Prevention of glycosaminoglycan accumulation in Hurler fibroblasts by rhIDU and RAP-IDU.** Fibroblasts were seeded in 6-well plates at 250,000 cells per well and labeled with [^{35}S]sulfate in the presence of rhIDU or RAP-IDU (both at 5 nM) for 48 h. Cells were then washed with PBS, lysed with NaOH, and assayed for radioactivity and total protein as described under "Experimental Procedures." *Inset*, 4–12% gradient Bis-Tris SDS-PAGE analysis of proteins used for the experiment, stained with Coomassie Blue. *Lane 1*, RAP-IDU; *lane 2*, rhIDU.

tained some key features of each fusion partner. The fusions bound to members of the LDLR family and were routed to the lysosome after being endocytosed. The fusions had appropriate enzymatic activity that was resistant to the conditions in the lysosome. GAA has been shown to undergo substantial N- and C-terminal proteolytic processing in the lysosome that would free it of any RAP or linker sequences (40). IDU has also been shown to be partly proteolyzed in the lysosome (41). Despite the difference in the molar specific activities of RAP-IDU and rhIDU, prevention of glycosaminoglycan storage in Hurler fibroblasts treated with RAP-IDU suggests that fusion-derived IDU was sufficiently active on heparin and dermatan sulfate, the natural substrates for this enzyme, to substitute for native enzyme.

The RAP-IDU fusion carried substantially less terminally phosphorylated high-mannose oligosaccharide (Bis-7) than the native enzyme, whereas the RAP-GAA fusion had no detectable phosphorylated oligosaccharide. Despite the diminished levels of phosphate, the RAP fusions were taken up into cells more efficiently than the corresponding, highly phosphorylated, enzymes.

A number of factors govern the uptake efficiency of phosphorylated enzyme and the corresponding RAP fusion. These include affinity for receptor, receptor density, receptor endocytosis rate, and receptor recycling rate. We have recently determined that the affinities of RAP-IDU and RAP-GAA for the LRP receptor are indistinguishable from the affinity of free RAP for the same receptor and are nearly identical to the affinity of phosphorylated enzyme for the MPR.[5] In contrast, the K_{uptake} values for the RAP fusions were about 25-fold higher than those of phosphorylated enzyme. K_{uptake} is a ratio defined as the sum of the off-rate constant for the receptor/ligand complex and the endocytic rate constant in the numerator and the on-rate constant for the receptor/ligand complex in the denominator. While K_{uptake} approaches K_d when the endocytic rate constant is small relative to the off-rate constant endocytic rate constants in the same range or greater than the off-rate constant will increase the K_{uptake} relative to K_d. Therefore, differences in the endocytic rate constants for lipoprotein receptors and the MPR may explain some of the difference in the K_{uptake} values for RAP fusions and phosphorylated enzymes. Another possibility is that the difference in apparent K_{uptake} is because of the participation of multiple receptor systems in endocytosis of the fusions. Previous studies of RAP uptake into fibroblasts have implicated a high capacity, low affinity receptor system as well as a low capacity, high affinity system, likely LRP (42). One candidate for the low affinity receptor is LDLR. LDLR is widely expressed and binds to RAP with a K_d of about 200 nM (36). Another candidate for the high capacity, low affinity receptor is cell-surface heparin sulfate proteoglycan, as RAP binds tightly to heparin (43). In addition to depressing the apparent K_{uptake} and elevating the system capacity for RAP and RAP fusion endocytosis, the lower affinity receptor would also be expected to obscure saturation of the higher affinity uptake receptor.

It is important that the RAP fusions effectively compete for receptor in the presence of high concentrations of other LDLR family ligands that are present in the blood. There is ample evidence of the unique receptor binding abilities of RAP in this regard. RAP antagonizes binding of a wide variety of ligands to LRP. Characteristics of this inhibitory effect are consistent with the induction of a receptor conformation change upon binding RAP that precludes subsequent binding of other ligands. There is also evidence that RAP can bind to portions of LRP that are bound by few other ligands, such as the third ligand binding domain of LRP1 (24). The unique receptor-binding behavior of RAP is consistent with the proposed role of this protein in blocking association of LRP receptors and LRP ligands within the complex mixture of proteins in the secretory pathway. These same properties might be expected to help RAP compete for receptor within the complex mixture of proteins in the circulatory system (23, 36, 44–46). The fact that only modest inhibition of fusion uptake was observed in the presence of 50% serum is consistent with the anticipated receptor-binding behavior of RAP in the face of competition from other LRP ligands.

The RAP sequence has a number of potential advantages over oligosaccharides in directing the efficient uptake and targeting of lysosomal enzymes to cells. The tissue distribution of

[5] Y. Wu, W. Lu, Y. Li, G. Bu, and T. C. Zankel, unpublished results; values were determined by solid-phase binding assay with an LRP receptor fragment comprising amino acids 833–954 of human LRP1.

the LDLR family as a whole is broad. The system capacity of the LDLR family, defined as the quantity of enzyme entering a cell in a particular interval of time, is considerably higher than that of the mannose 6-phosphate receptor in two unrelated cell types: primary fibroblasts and myoblasts, and modestly higher in a third cell type, C6 glioblastoma. System capacity depends on a number of variables including receptor density, affinity for ligand, and receptor recycling efficiency. The apparent affinity of the RAP fusions for LRP seems to be at least an order of magnitude lower than that of Bis-7 for MPR, yet RAP-mediated uptake of lysosomal enzyme exceeds mannose 6-phosphate-mediated uptake at all concentrations tested. Whereas many aspects of the receptor-dependent uptake of the RAP fusions remain to be defined, the implication of efficient RAP fusion uptake is significant for enzyme replacement therapy. More efficient uptake would potentially allow for lower doses or less frequent administration regimes.

Unlike the case for oligosaccharides, protein quality control mechanisms in the endoplasmic reticulum of mammalian cells ensure that all secreted RAP fusions are competent for uptake. This characteristic might simplify the manufacture and characterization of therapeutic proteins for ERT.

Finally, members of the LDLR family have been demonstrated to transcytose bound ligands across some polarized epithelial cells layers, including the blood-brain barrier endothelium (13, 15, 47–49). Lysosomal enzymes themselves, even in the phosphorylated form, have not been observed to cross the blood-brain barrier in quantities sufficient to correct the effects of lysosomal storage disorders. The trans-epithelial trafficking behavior of some LRP receptors might render certain tissues, such as the brain, accessible to RAP and to proteins that are fused to RAP, including lysosomal enzymes (37, 50–52). Bearing out this prediction, RAP itself was recently demonstrated to cross the blood-brain barrier (53). The distribution of intravenously administered RAP fusions to a variety of tissues, including the brain, is currently under study.

Acknowledgments—We thank Susan Flor, Simone Haslam, Diana Cheung, and Pavan Gulati for assay and cell culture support, Tri Do for help in purifying the fusions, and Jim Michaels, Isabelle Nadeau, Keri Mills, Alan Luk, and Marcus Curry for help in production of fusions.

REFERENCES

1. Kakkis, E. D. (2002) *Expert Opin. Investig. Drugs* **11,** 675–685
2. Zhao, K. W., Faull, K. F., Kakkis, E. D., and Neufeld, E. F. (1997) *J. Biol. Chem.* **272,** 22758–22765
3. Grabowski, G. A., Barton, N. W., Pastores, G., Dambrosia, J. M., Banerjee, T. K., McKee, M. A., Parker, C., Schiffmann, R., Hill, S. C., and Brady, R. O. (1995) *Ann. Intern. Med.* **122,** 33–39
4. Murray, G. J. (1987) *Methods Enzymol.* **149,** 25–42
5. Green, I., Christison, R., Voyce, C. J., Bundell, K. R., and Lindsay, M. A. (2003) *Trends Pharmacol. Sci.* **24,** 213–215
6. Xia, H., Mao, Q., and Davidson, B. L. (2001) *Nat. Biotechnol.* **19,** 640–644
7. LeBowitz, J. H., Grubb, J. H., Maga, J. A., Schmiel, D. H., Vogler, C., and Sly, W. S. (2004) *Proc. Natl. Acad. Sci. U. S. A.* **101,** 3083–3088
8. Argraves, W. S. (2001) *Front. Biosci.* **6,** D406–D416
9. Hussain, M. M., Strickland, D. K., and Bakillah, A. (1999) *Annu. Rev. Nutr.* **19,** 141–172
10. Herz, J., and Strickland, D. K. (2001) *J. Clin. Investig.* **108,** 779–784
11. Li, Y., Cam, J., and Bu, G. (2001) *Mol. Neurobiol.* **23,** 53–67
12. Li, Y., Lu, W., Marzolo, M. P., and Bu, G. (2001) *J. Biol. Chem.* **276,** 18000–18006
13. Marino, M., Zheng, G., Chiovato, L., Pinchera, A., Brown, D., Andrews, D., and McCluskey, R. T. (2000) *J. Biol. Chem.* **275,** 7125–7137
14. Chun, J. T., Wang, L., Pasinetti, G. M., Finch, C. E., and Zlokovic, B. V. (1999) *Exp. Neurol.* **157,** 194–201
15. Marino, M., Andrews, D., Brown, D., and McCluskey, R. T. (2001) *J. Am. Soc. Nephrol.* **12,** 637–648
16. Marzolo, M. P., Yuseff, M. I., Retamal, C., Donoso, M., Ezquer, F., Farfan, P., Li, Y., and Bu, G. (2003) *Traffic* **4,** 273–288
17. Li, Y., Lu, W., Schwartz, A. L., and Bu, G. (2002) *Biochemistry* **41,** 4921–4928
18. Bu, G. (2001) *Int. Rev. Cytol.* **209,** 79–116
19. Bu, G. (1998) *Curr. Opin. Lipidol.* **9,** 149–155
20. Andersen, O. M., Christensen, L. L., Christensen, P. A., Sorensen, E. S., Jacobsen, C., Moestrup, S. K., Etzerodt, M., and Thogersen, H. C. (2000) *J. Biol. Chem.* **275,** 21017–21024
21. Andersen, O. M., Schwarz, F. P., Eisenstein, E., Jacobsen, C., Moestrup, S. K., Etzerodt, M., and Thogersen, H. C. (2001) *Biochemistry* **40,** 15408–15417
22. Migliorini, M. M., Behre, E. H., Brew, S., Ingham, K. C., and Strickland, D. K. (2003) *J. Biol. Chem.* **278,** 17986–17992
23. Warshawsky, I., Bu, G., and Schwartz, A. L. (1993) *J. Clin. Investig.* **92,** 937–944
24. Obermoeller-McCormick, L. M., Li, Y., Osaka, H., FitzGerald, D. J., Schwartz, A. L., and Bu, G. (2001) *J. Cell Sci.* **114,** 899–908
25. Bu, G., Maksymovitch, E. A., and Schwartz, A. L. (1993) *J. Biol. Chem.* **268,** 13002–13009
26. Kakkis, E. D., Matynia, A., Jonas, A. J., and Neufeld, E. F. (1994) *Protein Expr. Purif.* **5,** 225–232
27. Horn, I. R., van den Berg, B. M., van der Meijden, P. Z., Pannekoek, H., and van Zonneveld, A. J. (1997) *J. Biol. Chem.* **272,** 13608–13613
28. Van Hove, J. L., Yang, H. W., Oliver, L. M., Pennybacker, M. F., and Chen, Y. T. (1997) *Biochem. Mol. Biol. Int.* **43,** 613–623
29. Fuller, M., Van der Ploeg, A., Reuser, A. J., Anson, D. S., and Hopwood, J. J. (1995) *Eur. J. Biochem.* **234,** 903–909
30. Starr, C. M., Masada, R. I., Hague, C., Skop, E., and Klock, J. C. (1996) *J. Chromatogr. A* **720,** 295–321
31. Hague, C., Masada, R. I., and Starr, C. (1998) *Electrophoresis* **19,** 2612–2620
32. Liu, C. X., Li, Y., Obermoeller-McCormick, L. M., Schwartz, A. L., and Bu, G. (2001) *J. Biol. Chem.* **276,** 28889–28896
33. FitzGerald, D. J., Fryling, C. M., Zdanovsky, A., Saelinger, C. B., Kounnas, M., Winkles, J. A., Strickland, D., and Leppla, S. (1995) *J. Cell Biol.* **129,** 1533–1541
34. Sando, G. N., and Neufeld, E. F. (1977) *Cell* **12,** 619–627
35. Iadonato, S. P., Bu, G., Maksymovitch, E. A., and Schwartz, A. L. (1993) *Biochem. J.* **296,** 867–875
36. Medh, J. D., Fry, G. L., Bowen, S. L., Pladet, M. W., Strickland, D. K., and Chappell, D. A. (1995) *J. Biol. Chem.* **270,** 536–540
37. Van der Ploeg, A. T., Kroos, M. A., Willemsen, R., Brons, N. H., and Reuser, A. J. (1991) *J. Clin. Investig.* **87,** 513–518
38. Yang, H. W., Kikuchi, T., Hagiwara, Y., Mizutani, M., Chen, Y. T., and Van Hove, J. L. (1998) *Pediatr. Res.* **43,** 374–380
39. Barton, R. W., and Neufeld, E. F. (1971) *J. Biol. Chem.* **246,** 7773–7779
40. Wisselaar, H. A., Kroos, M. A., Hermans, M. M., van Beeumen, J., and Reuser, A. J. (1993) *J. Biol. Chem.* **268,** 2223–2231
41. Myerowitz, R., and Neufeld, E. F. (1981) *J. Biol. Chem.* **256,** 3044–3048
42. Vassiliou, G., and Stanley, K. K. (1994) *J. Biol. Chem.* **269,** 15172–15178
43. Melman, L., Cao, Z. F., Rennke, S., Paz Marzolo, M., Wardell, M. R., and Bu, G. (2001) *J. Biol. Chem.* **276,** 29338–29346
44. Willnow, T. E., Sheng, Z., Ishibashi, S., and Herz, J. (1994) *Science* **264,** 1471–1474
45. Troussard, A. A., Khallou, J., Mann, C. J., Andre, P., Strickland, D. K., Bihain, B. E., and Yen, F. T. (1995) *J. Biol. Chem.* **270,** 17068–17071
46. Narita, M., Bu, G., Herz, J., and Schwartz, A. L. (1995) *J. Clin. Investig.* **96,** 1164–1168
47. Obunike, J. C., Lutz, E. P., Li, Z., Paka, L., Katopodis, T., Strickland, D. K., Kozarsky, K. F., Pillarisetti, S., and Goldberg, I. J. (2001) *J. Biol. Chem.* **276,** 8934–8941
48. Dehouck, B., Fenart, L., Dehouck, M. P., Pierce, A., Torpier, G., and Cecchelli, R. (1997) *J. Cell Biol.* **138,** 877–889
49. Zlokovic, B. V., Martel, C. L., Matsubara, E., McComb, J. G., Zheng, G., McCluskey, R. T., Frangione, B., and Ghiso, J. (1996) *Proc. Natl. Acad. Sci. U. S. A.* **93,** 4229–4234
50. Sands, M. S., Vogler, C. A., Ohlemiller, K. K., Roberts, M. S., Grubb, J. H., Levy, B., and Sly, W. S. (2001) *J. Biol. Chem.* **276,** 43160–43165
51. Kakkis, E. D., Schuchman, E., He, X., Wan, Q., Kania, S., Wiemelt, S., Hasson, C. W., O'Malley, T., Weil, M. A., Aguirre, G. A., Brown, D. E., and Haskins, M. E. (2001) *Mol. Genet. Metab.* **72,** 199–208
52. Shull, R. M., Kakkis, E. D., McEntee, M. F., Kania, S. A., Jonas, A. J., and Neufeld, E. F. (1994) *Proc. Natl. Acad. Sci. U. S. A.* **91,** 12937–12941
53. Pan, W., Kastin, A., Zankel, T. C., van Kerkhoff, P., Terasaki, T., and Bu, G. (2004) *J. Cell Sci.*, in press